THE JOURNAL OF BIOLOGICAL CHEMISTRY VOL. 285, NO. 17, pp. 13079–13091, April 23, 2010

Poly(ADP-ribose) Polymerase (PARP)-1-independent Apoptosis-inducing Factor (AIF) Release and Cell Death Are Induced by Eleostearic Acid and Blocked by α-Tocopherol and MEK Inhibition*[S]

Received for publication, July 14, 2009, and in revised form, February 2, 2010 Published, JBC Papers in Press, February 22, 2010, DOI 10.1074/jbc.M109.044206

Kazunari Kondo[‡1], **Saemi Obitsu**[‡], **Sayaka Ohta**[‡], **Katsuyoshi Matsunami**[§], **Hideaki Otsuka**[§], **and Reiko Teshima**[‡]

From the [‡]*Division of Novel Food and Immunochemistry, National Institute of Health Sciences, 1-18-1 Kamiyoga, Setagaya, Tokyo 158-8501 and the* [§]*Department of Pharmacognosy, Graduate School of Biomedical Sciences, Hiroshima University, 1-2-3 Kasumi, Minami-ku, Hiroshima 734-8553, Japan*

Poly(ADP-ribose)polymerase-1 (PARP-1) is thought to be required for apoptosis-inducing factor (AIF) release from mitochondria in caspase-independent apoptosis. The mechanism by which AIF is released through PARP-1 remains unclear. Here, we provide evidence that PARP-1-independent AIF release and cell death are induced by a trienoic fatty acid, α-eleostearic acid (α-ESA). α-ESA induced the caspase-independent and AIF-initiated apoptotic death of neuronal cell lines, independently of PARP-1 activation. The cell death was inhibited by the MEK inhibitor U0126 and by knockdown of MEK using small interfering RNA. However, inhibitors for JNK, p38 inhibitors, calpain, phospholipase A_2, and phosphatidylinositol 3-kinase, did not block cell death. AIF was translocated to the nucleus after the induction of apoptosis by α-ESA in differentiated PC12 cells without activating caspase-3 and PARP-1. The α-ESA-mediated cell death was not inhibited by PARP inhibitor 3,4-dihydro-5-[4-(1-piperidinyl)butoxyl]-1(2*H*)-isoquinoline and by knockdown of PARP-1 using small interfering RNA. Unlike *N*-methyl-*N*′-nitro-*N*-nitrosoguanidine treatment, histone-phosphorylated histone 2AX was not phosphorylated by α-ESA, which suggests no DNA damage. Overexpression of Bcl-2 did not inhibit the cell death. α-ESA caused a small quantity of superoxide production in the mitochondria, resulting in the reduction of mitochondrial membrane potential, both of which were blocked by a trace amount of α-tocopherol localized in the mitochondria. Our results demonstrate that α-ESA induces PARP-1-independent AIF release and cell death without activating Bax, cytochrome *c*, and caspase-3. MEK is also a key molecule, although the link between ERK, AIF release, and cell death remains unknown. Finding molecules that regulate AIF release may be an important therapeutic target for the treatment of neuronal injury.

Apoptosis is a mode of programmed cell death that is used by multicellular organisms to remove surplus and unwanted cells in the immune and nervous systems (1–5). Apoptosis is characterized by cell detachment, cell shrinkage, chromatin condensation, DNA degradation, and plasma membrane blebbing (5–7). The surplus cells are removed by caspases, which are key effector molecules of apoptotic cell death. Apoptosis is activated through two main pathways as follows: the extrinsic pathway, which originates from the activation of cell-surface death receptors, such as Fas and tumor necrosis factor-receptor 1, and results in the activation of caspase-8; and the intrinsic pathway, which originates from the mitochondrial release of cytochrome *c* and results in the activation of caspase-9 through the Cyt-c[2]/apoptotic protease-activating factor-1/procaspase-9 heptamer (5, 8, 9). Most apoptotic stimuli use a mitochondrion-dependent process such as membrane potential shutdown and outer membrane permeabilization controlled by Bax and Bak, which are pro-apoptotic members of the Bcl-2 family (6–9). This results in the release of the pro-apoptotic protein Cyt-c, which triggers caspase activation, or the apoptosis-inducing factor (AIF), which triggers caspase-independent pathways, from mitochondrial intermembrane space.

In the developing nervous system, apoptosis is necessary for the establishment of appropriate cell numbers and for the elimination of unwanted cells (10); however, in the adult nervous system, the inappropriate induction of apoptotic cell death contributes to neurodegenerative diseases (15, 16). Activation of the mitochondrial signaling cascade can activate both caspase-dependent and caspase-independent apoptosis (11, 12). AIF is a key molecule in caspase-independent neuronal cell death (13–16). AIF is released from the mitochondria into the cytosol and then translocated to the nucleus in response to neuronal

* This work was supported by grants from the Ministry of Health, Labor, and Welfare of Japan, the Japan Health Sciences Foundation, and Grant-in-aid for Scientific Research 20590132 (to K. K.).

[S] The on-line version of this article (available at http://www.jbc.org) contains supplemental Figs. S1 and S2 and Movie S1.

[1] To whom correspondence should be addressed. Tel.: 81-3-3700-1141; E-mail: kondo@nihs.go.jp.

[2] The abbreviations used are: Cyt-c, cytochrome *c*; α-ESA, α-eleostearic acid; MEK, mitogen-activated protein kinase kinase; JNK, c-Jun N-terminal kinase; ERK, extracellular signal-regulated kinase; γ-H2AX, phosphorylated histone 2AX; AIF, apoptosis-inducing factor; Bak, Bcl-2-antagonist/killer; Bax, Bcl-2-associated X protein; CPT, camptothecin; DPQ, 3,4-dihydro-5-[4-(1-piperidinyl)butoxyl]-1(2*H*)-isoquinoline; ERK, extracellular signal-regulated kinase; MEK, mitogen-activated protein kinase kinase; MNNG, *N*-methyl-*N*′-nitro-*N*-nitrosoguanidine; NGF, nerve growth factor; PARP-1, poly(ADP-ribose) polymerase-1; Z-, *N*-benzyloxycarbonyl; fmk, fluoromethyl ketone; ROS, reactive oxygen species; α-ESA, α-eleostearic acid; Ab, antibody; siRNA, small interfering RNA; TUNEL, terminal dUTP nick end-labeling; α-Toc, α-tocopherol; NMDA, *N*-methyl-D-aspartic acid; STS, staurosporine; JNK, c-Jun N-terminal kinase; PAR, polymer of ADP-ribose; CM-H2DCF-DA, 5(and 6)-chloromethyl-2′,7′-dichlorodihydrofluorescein diacetate; NBD, 7-nitro-2,1,3-benzoxadiazol-4-yl.

stimuli, including hypoxia, cerebral ischemia, and *N*-methyl-*N*′-nitrosoguanidine (MNNG) or *N*-methyl-D-aspartic acid (NMDA) insult (15, 17–20). Poly(ADP-ribose) polymerase-1 (PARP-1) activation is required for the translocation of AIF in fibroblasts (20). Moubarak *et al.* (21) has reported that the sequential activation of PARP-1, calpain, and Bax is essential in AIF-mediated programmed necrosis.

α-Eleostearic acid (α-ESA) is a conjugated trienoic fatty acid that occurs in the seeds of plants such as *Vernicia* spp. α-ESA has been reported to suppress tumor growth through caspase-3 and peroxisome proliferator-activated receptor-γ activation accompanied by DNA fragmentation (22–24). Recently, we have found that α-ESA induces caspase-independent apoptosis that is not associated with nucleosomal DNA fragmentation in neuronal cells. Notably, α-ESA-mediated apoptotic cell death is accompanied by AIF translocation to the nucleus and prolonged ERK phosphorylation that lasts for more than 16 h, but not by PARP-1 activation, in rat adrenal pheochromocytoma PC12 cells. The MEK inhibitor U0126 and a trace amount of α-tocopherol (α-Toc) completely inhibited the apoptotic cell death. The methyl ester of α-ESA (α-ESA-Me) did not induce apoptotic cell death, even though it has the same conjugated triene group as α-ESA. Here, we show that α-ESA causes PARP-1-independent AIF release and the cell death through the superoxide production in a small quantity in the mitochondria and the prolonged ERK1/2 phosphorylation without inducing other apoptotic molecules such as Bax, Bcl-2, Cyt-c, caspase-3, and PARP-1.

EXPERIMENTAL PROCEDURES

Cell Culture—PC12 (JCRB0266) cells were grown in Dulbecco's modified Eagle's medium supplemented with 10% horse serum and 5% fetal calf serum, penicillin, and streptomycin (Invitrogen). Human neuroblastoma (SH-SY5Y) cells (American Type Culture Collection (ATCC), CRL-2266) were grown in Dulbecco's modified Eagle's medium/F-12 supplemented with 10% fetal calf serum. Mouse neuroblastoma × rat glioma hybrid (NG108-15) cells (ATCC, HB-12317) were grown in Dulbecco's modified Eagle's medium supplemented with 10% fetal calf serum. The PC12 cells were induced to differentiate by treatment with 50 ng/ml NGF 7 S (Sigma) and were maintained at 37 °C and 5% CO_2. The SH-SY5Y and NG108-15 cells were induced to differentiate by treatment with 10 μM all-*trans*-retinoic acid (Sigma) and 250 μM dibutyryl cyclic AMP (Tocris), respectively. The PC12 and NG108-15 cells were allowed to differentiate on polylysine-coated plates or glass chambers. The cell viability was measured by a WST-8 assay (Nacalai Tesque, Japan). Briefly, PC12 cells were differentiated by NGF for 48 h, and then α-ESA was added to the cells. Sixteen hours later, the cell count reagent (2-(2-methoxy-4-nitrophenyl)-3-(4-nitrophenyl)-5-(2,4-disulfophenyl)-2*H* tetrazolium) for the WST-8 assay was added to the cells, and the cells were incubated for 1–2 h. For proliferating cells, α-ESA was added 16–18 h after seeding the cells. Cell viability was measured by 450 and 650 nm (as a reference) absorbance. When pretreatment with a specific inhibitor is needed, an inhibitor was added to the cells 30 min before α-ESA. Cell viability data were obtained between two and four independent experiments performed in triplicate.

Antibodies and Chemicals—The Abs for ERK, phospho-ERK, JNK/stress-activated protein kinase, phospho-JNK/stress-activated protein kinase, p38, phospho-p38, Akt, phospho-Akt, caspase-3, MEK1 (61B12), Bcl-2, and glyceraldehyde-3-phosphate dehydrogenase (14C10) were purchased from Cell Signaling. The Abs for AIF (E-1), Cyt-c (7H8), Bax (N-20), Bcl-2 (C-2), and PARP-1 (H-250) were purchased from Santa Cruz Biotechnology. Anti-PAR (10H) was obtained from Alexis Biochemicals. Anti-H2A was obtained from Millipore. Anti-γ-H2AX was obtained from Active Motif. Anti-manganese superoxide dismutase was obtained from Assay Designs. Anti-MEK2 was purchased from BD Biosciences. The pan-caspase inhibitor Z-VAD-fmk, PD98059, SB203580, U0126, palmitoyl trifluoromethyl ketone, and DPQ were obtained from Calbiochem. SP600125 was obtained from Assay Designs. 7-Nitro-2,1,3-benzoxadiazol-4-yl (NBD)-labeled α-Toc was kindly provided by J. Atkinson (Brock University, Canada). Bromoenol lactone and methylarachidonyl fluorophosphates were purchased from Cayman Chemicals. The orange fluorescent protein-tagged leader sequence of E1α pyruvate dehydrogenase (Organelle Light), MitoTracker Red CM-H2Ros, and MitoSOX Red were purchased from Invitrogen and used to stain with the mitochondria. The high purity of α-ESA was purchased from Larodan Fine Chemicals (Sweden). Staurosporine was obtained from Tocris Bioscience. 5(and 6)-Chloromethyl-2′,7′-dichlorodihydrofluorescein diacetate (CM-H2DCF-DA) was purchased from Invitrogen. BESSo-AM was purchased from Wako Pure Chemicals (Japan). α-ESA-Me was prepared by reacting α-ESA with trimethylsilyl-diazomethane in 10% hexane solution (TCI, Japan). Trimethylsilyl-diazomethane was added to the reaction mixture (α-ESA, 20.0 mg in 18 ml methanol) drop-by-drop over 1 h at room temperature to avoid by-products. The reaction mixtures were purified with a C_{18} column. The resulting material was stored in a vial under a nitrogen gas atmosphere at −80 °C or below.

Western Blot Analysis—PC12 cells were cultured at 6×10^5 cells/dish in 10-cm poly-L-lysine-coated dishes in a differentiation condition. After 24 h, the cells were cultured with NGF for another 48 h. α-ESA was then added to the cells to induce apoptosis after inhibitors, U0126 or α-Toc, if needed. The cells were collected after 16 h of α-ESA treatment. Briefly, after the cells were washed with Tris-buffered saline, lysates were prepared using Triton-based lysis buffer containing protease inhibitors and phosphatase inhibitors. Neurotropic factor (NGF) was included in the washing buffer to avoid other types of apoptosis caused by neurotropic factor withdrawal from differentiating cells. A ProteoExtract subcellular proteome extraction kit (Calbiochem) was used for the preparation of the nuclear and cytosolic fractions. The cell lysates and subcellular fraction samples were resolved by SDS-PAGE on 5–20% gradient gels and transferred onto polyvinylidene fluoride membranes (ATTO, Japan). The membranes were incubated with primary Abs at 4 °C overnight and then with alkaline phosphatase-labeled secondary Abs for 1 h at room temperature. The blots were detected by an alkaline phosphatase-conjugated substrate kit (Bio-Rad). For Bcl-2 overexpression and siRNA experiments, a chemiluminescent ECL system was used to

detect the blots. Western blot analyses were performed on data from more than three independent experiments.

Immunofluorescent Staining—PC12 cells on poly-L-lysine-coated glass chamber slides were washed twice with Dulbecco's phosphate-buffered saline containing NGF before the cells were fixed with 4% paraformaldehyde (Wako, Japan) for 30 min and permeabilized with cold 0.2% Triton X-100 for 10 min. After blocking with 2% bovine serum albumin for 1 h, the cells were incubated with primary Abs against Bax, AIF, ERK, or phospho-histone H2AX at 4 °C overnight. The cells were washed and incubated with Alexa 488- or Texas Red-labeled secondary antibodies (Invitrogen) and Hoechst 33342 (Invitrogen) or TUNEL (Roche Diagnostics) at room temperature for 1 h. After washing, the cells were mounted with Prolong gold mounting media (Invitrogen). Fluorescent microscopy was performed using an IX71 microscope (Olympus, Japan), a deconvolution microscope DeltaVision personal DV (Applied Precision), and a Leica confocal microscope TCS-SP5 (Leica Microsystems, Germany). Immunofluorescent staining data were obtained from more than four independent experiments.

Caspase-3/7 Assay—PC12 cells were cultured in 10-cm poly-L-lysine-coated dishes in the differentiation condition. The caspase-3 activity of lysates from PC12 cells treated with ESA was measured with the Apo-ONE homogeneous caspase-3/7 assay kit (Promega) according to the manufacturer's protocol using a fluorescent plate reader (Infinity M, Tecan). Data were obtained from two independent experiments.

DNA Analysis—Genomic DNA was extracted from the cells treated with α-ESA for 30 h using FastPure DNA kit (Takara, Japan), and DNA was analyzed using agarose gel electrophoresis and pulse field gel electrophoresis (CHEF DR-II, Bio-Rad). The conditions for the pulse field gel electrophoresis were as follows: 1% agarose, 6 V/cm, 15 °C, 15 h.

Bcl-2 Transfection—The human *bcl-2* was a kind gift from Y. Tsujimoto (Osaka University, Japan). The *bcl-2* was subcloned into the pcDNA-DEST40 expression vector (Invitrogen). PC12 cells (2×10^6 cells/ml) were transfected with the *bcl-2* by an electroporation method (Amaxa Nucleofector II; Lonza, Switzerland) according to the manufacturer's protocol (program U-029). The same numbers of the transfected cells were seeded to 35-mm dishes in the differentiation condition. Twenty four hours after the transfection, the cells were exposed to α-ESA for an additional 24 h. The cell viability was then measured using the WST-8 reagent, and Western blot analysis was performed to check Bcl-2 protein expression. Blots were detected using ECL plus (GE Healthcare) and Hyperfilm (GE Healthcare) following horseradish peroxidase-labeled secondary Abs.

RNA Interference—The knockdown of PARP-1 was performed in PC12 cells using predesigned ON-TARGET*plus* siRNA SMART pool purchased from Dharmacon. The transfection efficiencies were optimized using siRNA optimization kit (Amaxa). The transfections were performed by the electroporation method (Amaxa, program U029), and the same numbers of the transfected cells were seeded to 35-mm dishes. After 24 h of incubation in the differentiation condition, the cells were exposed to α-ESA or MNNG (500 μM, 15 min) for an additional 24 h. ON-TARGET*plus* nontargeting siRNA pool (300 nM) was used as a control for nonsequence-specific effects. The knockdown of MEK1/2 was performed using predesigned Stealth Select siRNA (1 μM) purchased from Invitrogen. Two mixed primers for each target (MEK1 or MEK2) were used for the experiments. Map2k1-RSS301293 and -RSS301295 are for MEK1. Map2k2-RSS339849 and -RSS339850 are for MEK2 (Invitrogen). Stealth RNA interference negative control was used as a control for nonsequence-specific effects. The cell viability was then measured using the WST-8 reagent, and Western blot analysis was performed to check protein expression. The blots were detected using ECL Plus (GE Healthcare) or an alkaline phosphatase-conjugated substrate kit (Bio-Rad).

Microinjection of AIF Antibody—AIF antibody (100 μg/ml, mouse IgG2b) or MOPC21 (100 μg/ml, isotype control for IgG2b) was microinjected into the differentiated PC12 cells using Stamporation apparatus SU100 (Olympus, Japan) and StampoNeedle (ST-ME330CN-20A, Olympus) (25) in 35-mm poly-L-lysine-coated culture dishes. The microinjected cells were exposed to α-ESA (2 μg/ml) after a 6-h incubation. After 16 h of treatment with α-ESA, the cells were stained with propidium iodide.

Bax Localization—The differentiated PC12 cells were treated with staurosporine (STS, 500 nM) or α-ESA (2 μg/ml). The cells were fixed and stained with Bax and MitoTracker Red CM-H2XRos (1 μM).

Measurements of ROS and Potential—Intracellular ROS and mitochondrial superoxides were measured using H2DCF-DA (10 μM) and MitoSOX Red (5 μM), respectively. Differentiated PC12 cells were incubated with CM-H2DCF-DA or MitoSOX for 1 h or 10 min, respectively. After washing, α-ESA was added to the cells. After 2, 5, and 20 h of incubation, the cells were counted to calculate the percentages of ROS-positive cells from a total of 100 cells. Cells that have fluorescent intensities more than the signal to noise ratio of >5 were determined to be positive. ImageJ (version 1.41) software was used to analyze the intensities of the cells. Mitochondrial membrane potential was measured using JC-1 (5 μM).

Statistical Analysis—All data are expressed as the mean ± S.D. The statistical significance was evaluated by one-way analysis of variance followed by the Dunnett's test to compare the data from multiple groups against a common control group (SigmaPlot). Student's *t* test was used to compare the data from two groups. Statistical significance was determined at $p < 0.05$ (indicated with an *asterisk* in the figures).

RESULTS

α-ESA Induces Apoptosis in Neuronal Cells—The time course illustration of the experiments using α-ESA (Fig. 1*A*) were shown with the morphological and nuclear changes in Fig. 1*B*. In both proliferating (nondifferentiated) and differentiated cells, apoptotic cell death was initiated. PC12 cells were seeded 18 h before the addition of NGF. NGF induced strong ERK1/2 phosphorylation between 7 min and 1 h, resulting in the differentiation and neurite outgrowth. Forty eight hours after the addition of NGF, the phosphorylation of ERK1/2 decreased to the basal level. Then α-ESA (2 μg/ml) was added to the differentiated PC12 cells (Fig. 1*C*). α-ESA induced apoptotic cell death in a dose-dependent manner in neuronal PC12, SH-SY5Y, and NG108-15 cells (Fig. 1*D*). The α-ESA-mediated

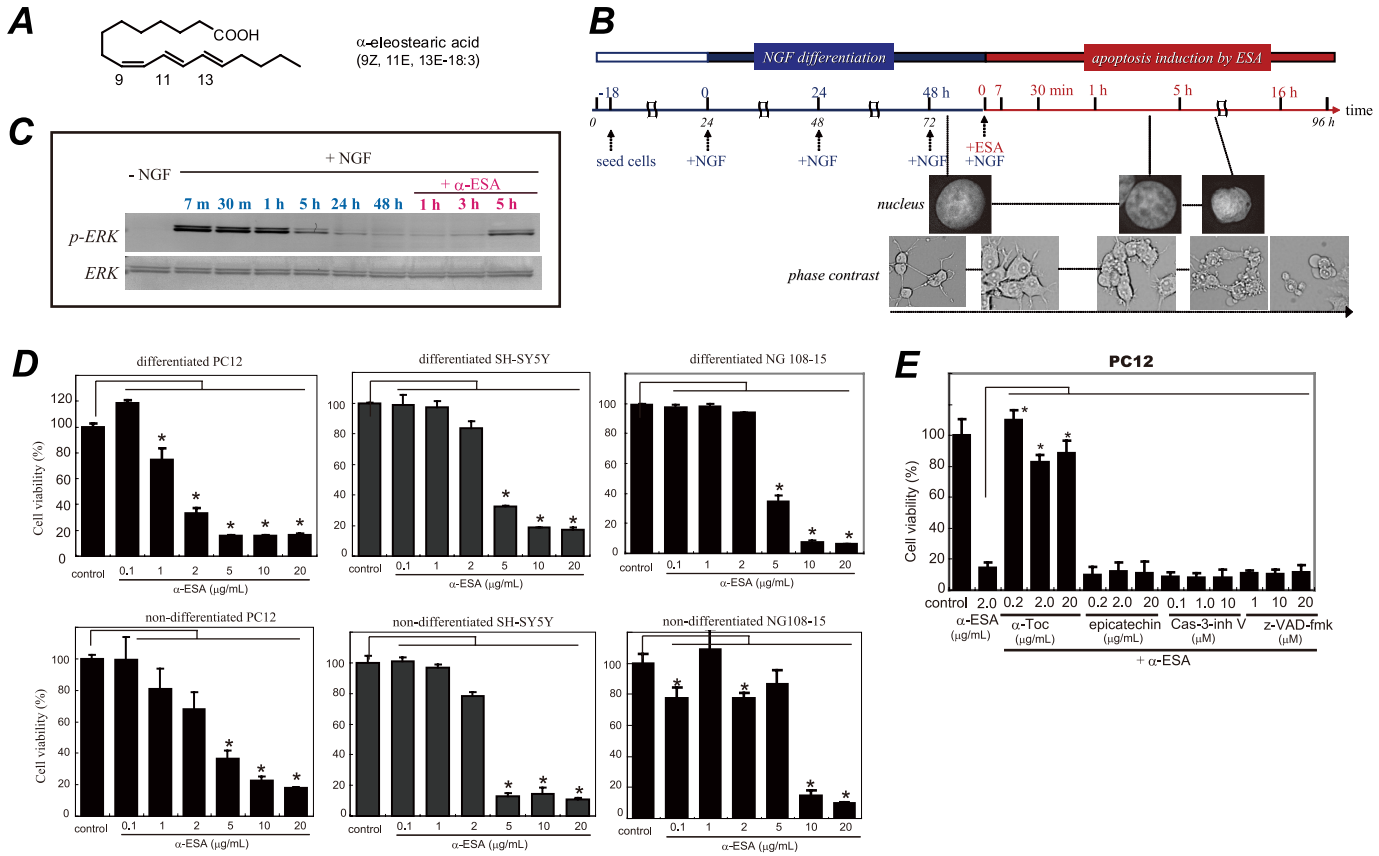

FIGURE 1. **α-ESA induces apoptotic cell death in neuronal cells.** *A*, structure of α-ESA. *B*, time course of α-ESA-mediated cell death in the differentiated PC12 cells. The cells were differentiated by NGF for 48 h and then exposed to α-ESA. *C*, time course of phosphorylation of ERK1/2 during NGF and α-ESA treatment. NGF induced a strong phosphorylation of ERK1/2, and its phosphorylation decreased to the basal level by 48 h. Then the addition of α-ESA induced prolonged and moderate phosphorylation of ERK1/2 again, resulting in the cell death. *D*, α-ESA (2 μg/ml) induced apoptotic cell death in neuronal PC12, SH-SY5Y, and NG108-15 cells. $n = 9$; $p < 0.05$ *versus* control (DMSO alone). *E*, α-ESA-mediated apoptosis was not inhibited by pan-caspase inhibitor Z-VAD-fmk and caspase-3 inhibitor in PC12 cells. α-Toc, but not epicatechin, inhibited the cell death. The values represent the means ± S.D. The viability of α-ESA treated cells was measured by WST-8 reagent 16 h after the treatment. *, $p < 0.05$.

cell death was not inhibited by the pan-caspase inhibitor Z-VAD-fmk and caspase-3 inhibitor V (Z-D(OMe)QM-D(OMe)-fmk) (Fig. 1*E*). Methyl ester of α-ESA did not induce cell death (supplemental Fig. S1).

Effects of MAPK Inhibitors and Antioxidants on α-ESA-mediated Cell Death—A variety of inhibitors was tested to clarify the mechanisms by which α-ESA provoked apoptotic cell death (Fig. 2 and supplemental Fig. S1). The MEK1/2 inhibitor U0126, which inhibits MEK1/2 activity and thereby blocks ERK1/2 phosphorylation, completely abrogated the α-ESA-mediated cell death at a concentration of 5 μM in both nondifferentiated and differentiated cells (Fig. 2*A*). The suppression of phosphorylated ERK1/2 may be important. The cell death was not inhibited by the c-Jun N-terminal kinase (JNK) inhibitor SP600125 and the p38 inhibitor SB203580 (Fig. 2*B*).

Next, the effect of antioxidants on the α-ESA-mediated cell death was examined. Cell death was fully abrogated by α-Toc in neuronal PC12 cells (Fig. 2*C*) but was not inhibited by the green tea antioxidant epicatechin (Fig. 1*E*). Other antioxidants, such as flavonoids (including quercetin and luteolin) and β-carotene, did not reduce the α-ESA-mediated cell death.[3] A trace amount (0.01 μg/ml; equivalent to 23 nM) of α-Toc significantly blocked the cell death induced by 2 μg/ml (equivalent to 7.2 μM) α-ESA (Fig. 2*C*). The inhibitory effects of U0126 and α-Toc on the α-ESA-mediated cell death were also observed in SH-SY5Y and NG108-15 cells (Fig. 2*D*). These results suggest that the α-ESA-mediated cell death is not dependent on neurotropic factors such as NGF, retinoic acid, or dibutyryl-cAMP. Thus, ERK1/2 and α-Toc appear to be a key molecule in the α-ESA-mediated apoptotic cell death.

Transient activation of ERK1/2 occurred when PC12 cells were treated with epidermal growth factor, and sustained activation of ERK1/2 occurred when the cells were treated with NGF (26, 27). After NGF stimulation for a few hours, the sustained ERK1/2 phosphorylation decreased to the basal level in our experiments (Fig. 1*C*). α-ESA was then added to the culture media containing NGF, and the ERK1/2 phosphorylation was investigated at variable intervals in PC12 cells (Fig. 3). Similar experiments were performed in the cells that were pretreated with the MEK1/2 inhibitor U0126 or α-Toc for 30 min. Prolonged ERK1/2 phosphorylation that lasted for at least 16 h was observed in the α-ESA-treated PC12 cells as well as in the camptothecin (CPT)-treated cells. ERK1/2 phosphorylation was observed 2–6 h after the addition of α-ESA and strongly increased by 16 h. U0126 blocked the ERK1/2 phosphorylation

[3] K. Kondo, S. Obitsu, S. Ohta, K. Matsunami, H. Otsuka, and R. Teshima, unpublished data.

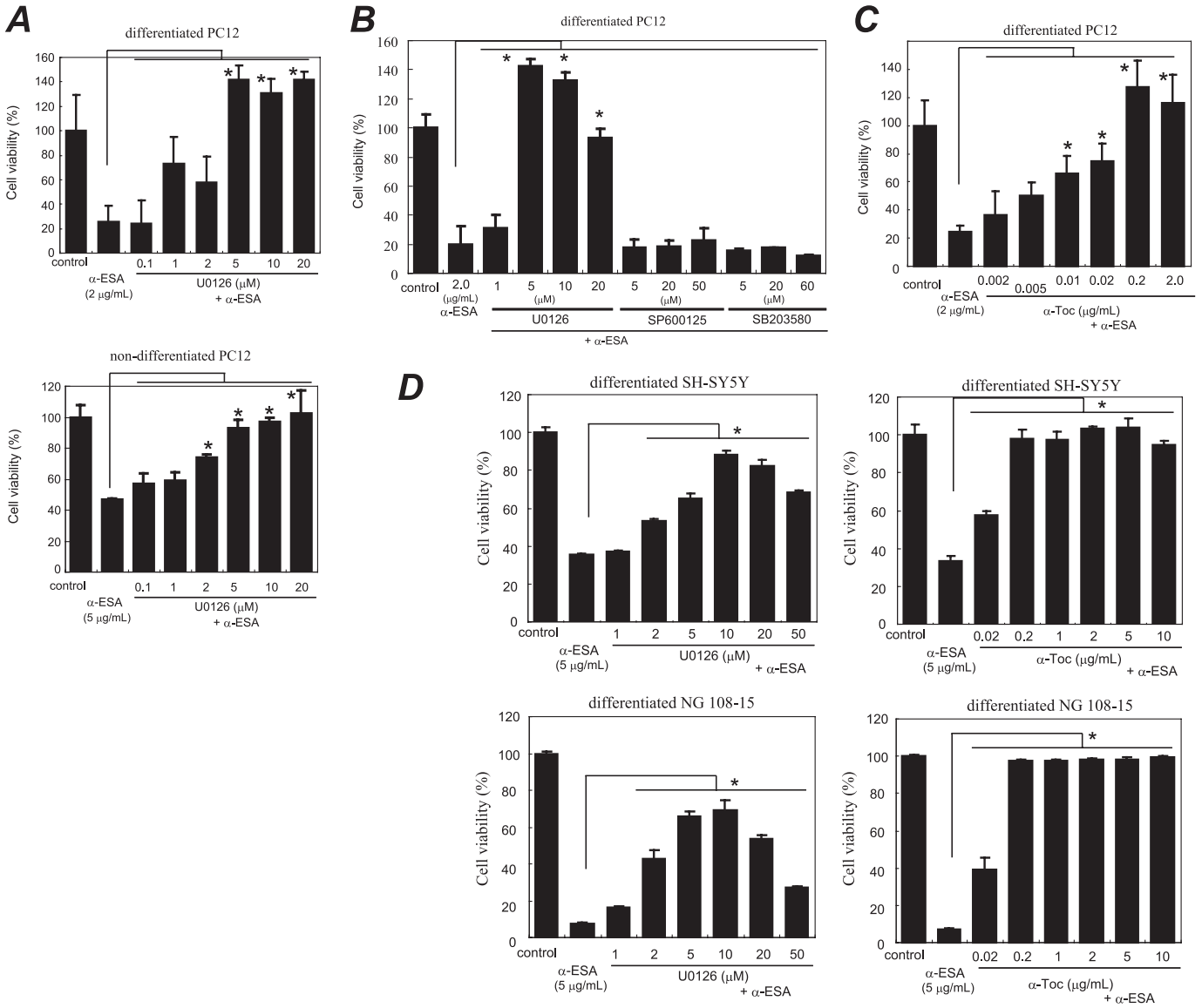

FIGURE 2. **MEK inhibitor and α-tocopherol block α-ESA-mediated cell death.** *A,* MEK inhibitor U0126 prevented α-ESA-mediated cell death in both differentiated and nondifferentiated PC12 cells (5 or 2 μM). $n = 6$; *, $p < 0.05$ *versus* α-ESA alone. *B,* JNK inhibitor SP600125 and p38 inhibitor SB203580 did not block α-ESA-mediated cell death. *C,* α-Toc blocked α-ESA-mediated cell death at lower concentrations (0.01 μg/ml). $n = 6$; *, $p < 0.05$ *versus* α-ESA alone. *D,* in both SH-SY5Y and NG108-15 cells, α-ESA-mediated cell death was blocked by U0126 and α-Toc. The values represent the means ± S.D. The viability of α-ESA treated cells was measured by WST-8 16 h after the treatment.

and thereby prevented the α-ESA-mediated cell death. In contrast, the ERK1/2 phosphorylation was not inhibited by α-Toc, although it completely prevented the cell death (Fig. 3, *A* and *D*). U0126 did not prevent the CPT-initiated apoptosis.[3] These results suggest that the inhibitory mechanism of α-Toc differs from that of U0126.

Next, we examined the activation of caspase-3 during the α-ESA-mediated apoptosis. Caspase-3 was not cleaved to yield an active fragment by α-ESA stimulation over a 16-h time course (Fig. 3*A*). The enzyme activity of caspase-3 was also measured using the fluorescent substrate bis-(*N*-benzyloxycarbonyl-L-aspartyl-L-glutamyl-L-valyl-aspartic acid amide)-rhodamine 110 (Z-DEVD-rhodamine 110). The activity of caspase-3 markedly increased in the CPT-treated cells, whereas no increase in the caspase-3 activity was observed in the α-ESA-treated cells (Fig. 3*B*). CPT was used as a positive control of caspase-3 activation.

ERK1/2 translocation to the nucleus was investigated using confocal microscopy. ERK1/2 migrated to the nucleus 4 h after the induction of apoptotic cell death by α-ESA (Fig. 3*C*). *YZ* planar images confirmed that ERK1/2 was localized in the nucleus. This result was consistent with Western blot analysis data. Actin rearrangement was abrogated in PC12 cells treated with α-ESA. The growth cone of neurite of the cells was significantly suppressed, showing the retardation of pseudopods.

AIF Translocation to the Nucleus and Chromatin Condensation—We next investigated AIF migration upon α-ESA treatment. ERK1/2 was localized in the nucleus when PC12 cells were treated with α-ESA as described above. AIF was initially localized in the mitochondria and migrated to the

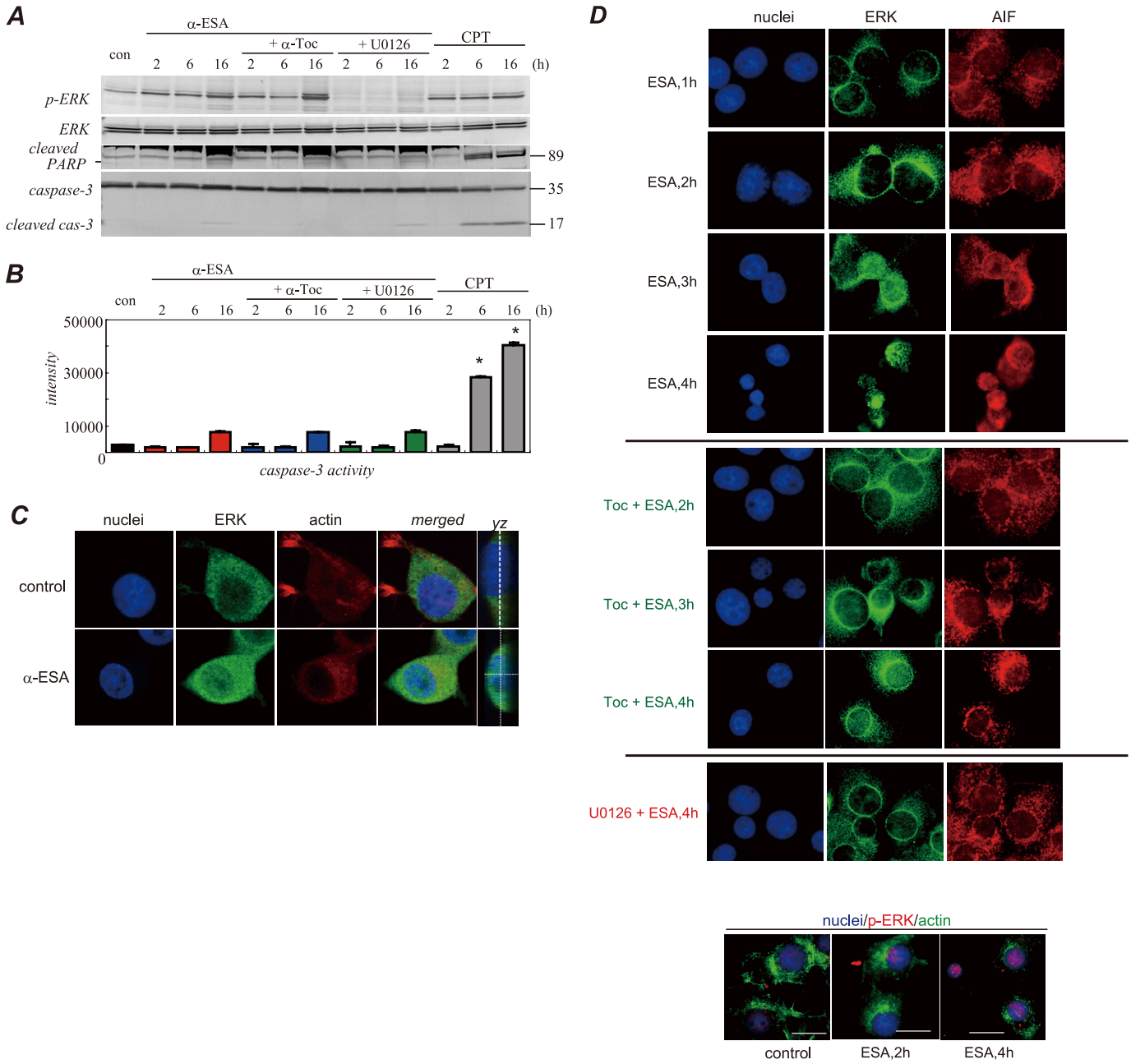

FIGURE 3. **ERK1/2 phosphorylation, PARP-1, and caspase-3 activation induced by α-ESA.** *A,* Western blot samples were prepared from PC12 cells at different time points (2, 6, and 16 h). Western blot analysis was independently repeated three times, and representative data are shown here. ERK1/2 was phosphorylated 2 h or later after α-ESA treatment. U0126 blocked the phosphorylation, whereas α-Toc did not. The cleaved form of PARP-1 (89 kDa) and the active form of caspase-3 (17 kDa) were not detected in α-ESA-treated cells. *con,* control. *B,* caspase-3 enzymatic activity was measured using a fluorescent substrate. The activity remained at the basal level until 6 h after the induction of apoptosis by α-ESA. CPT was used as a positive control of caspase-3 activity. *, $p < 0.05$ *versus* control (DMSO alone). *C,* ERK1/2 migrated to the nucleus upon α-ESA treatment. Images were obtained from samples treated with α-ESA for 4–5 h. Growth cone disappeared, and the actin rearrangements were suppressed. The confocal microscopy images showed that ERK1/2 was localized throughout the nucleus. *D,* treatment of U0126, but not α-Toc, blocked nuclear localization of ERK1/2. The nuclear localization of ERK1/2 and AIF was observed in the α-ESA-mediated cells. Phosphorylated ERK1/2 was observed in the nucleus (*bottom panel*).

nucleus upon α-ESA treatment. At 4 h after the induction of apoptotic cell death, AIF was translocated from the mitochondria to the nucleus, and the number of TUNEL-positive cells was increased. By 7 h after the induction of apoptosis, AIF was mostly localized in the nucleus and DNA compaction occurred (Fig. 4*A*). It was previously reported that when caspase-independent apoptosis was induced, AIF caused the cleavage of DNA into large fragments (~50 kb), which was referred to as stage-I apoptosis (28). Similar DNA cleavage was observed in the α-ESA-treated cells, which was not associated with nucleosomal DNA fragmentation. Pulse field gel electrophoresis revealed the cleavage of DNA into large scale (30–50 kb) fragments in neuronal PC12 cells (Fig. 4*B*). In deconvolution analysis, 30 slices of images were obtained to rebuild three-dimensional images. Data analysis was done using ImageJ software. This result clearly shows AIF localization in the nucleus and the TUNEL-positive nucleus. The subcellular fractions were analyzed by Western blotting. AIF was released from the mito-

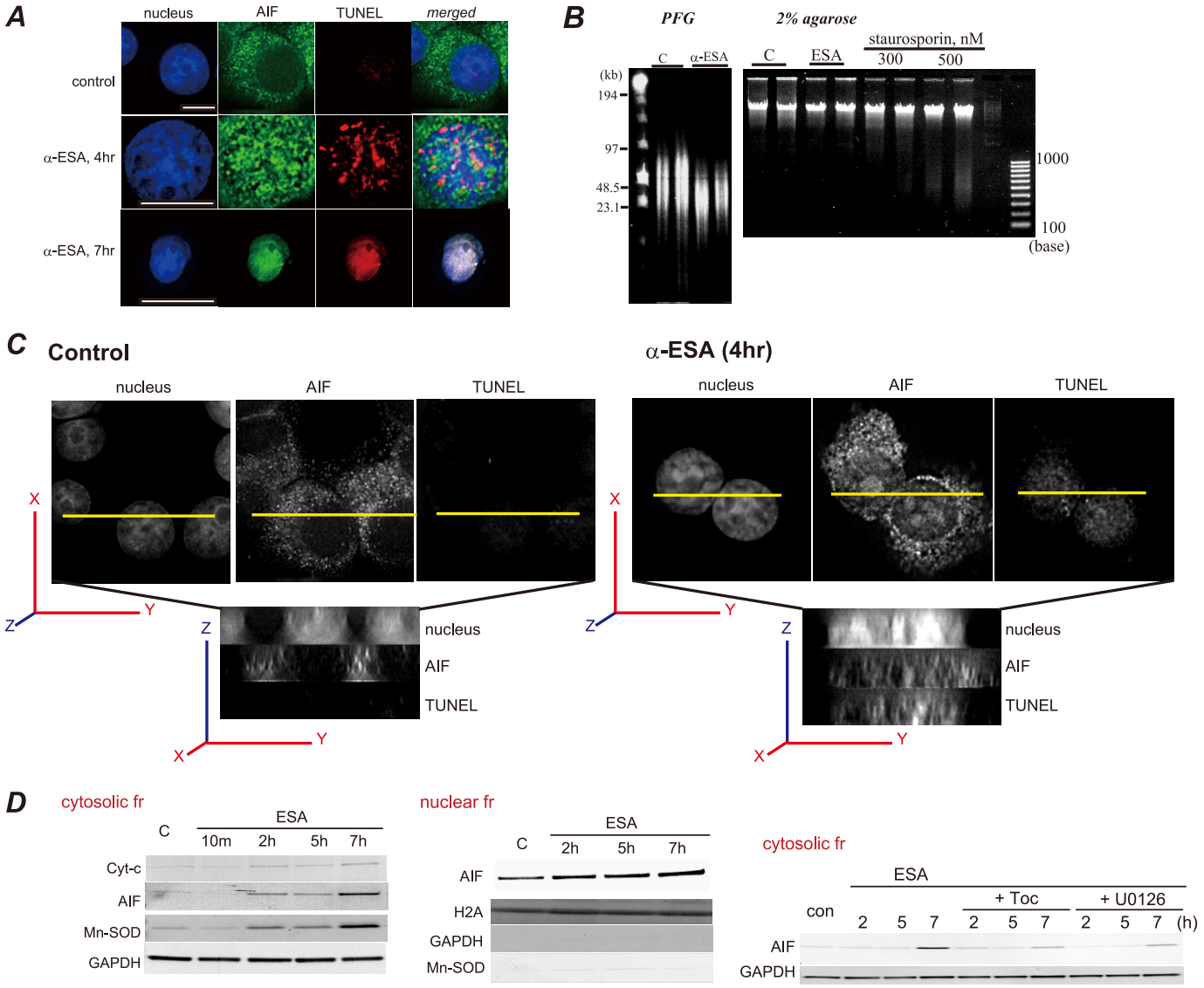

FIGURE 4. **AIF translocation to the nucleus by α-ESA.** *A,* α-ESA induced AIF translocation from the mitochondria to the nucleus. At 4 h after the induction of apoptosis by α-ESA, AIF was translocated to the nucleus (*green*). The nucleus was stained with TUNEL (*red*) and Hoechst (*blue*). *Scale bars* show 10 μm. The TUNEL staining was scattered. By 7 h, the nucleus greatly condensed, and AIF spread throughout the nucleus. The peripheral distribution of chromatin in the α-ESA-treated cell shown was characteristic of AIF-induced stage-I condensation. Images were obtained using the deconvolution microscope. *B,* DNA analysis. Genomic DNA was extracted from PC12 cells that were treated with either DMSO as a control or α-ESA (2 μg/ml) for 30 h. The extracted DNA was analyzed by pulse field gel (*PFG*) electrophoresis. High molecular weight fragments (30–50 kb) were detected on pulse field electrophoresis. Nucleosomal DNA fragmentation was analyzed by 2% agarose gel, showing that α-ESA did not induce nucleosomal DNA degradation. *C,* three-dimensional images of AIF localization in the nucleus. AIF was localized in the whole nucleus, and the nucleus was stained with TUNEL. *D,* subcellular fractionation analysis. The release of AIF and manganese superoxide dismutase (*Mn-SOD*) was observed in the cytosolic fraction (*fr*) of α-ESA-treated cells, resulting in AIF-initiated cell death (*left panel*). The Western blotting of the nuclear fraction revealed AIF localization in the nucleus. There is no contamination of cytosolic and heavy membrane fractions, including mitochondria. α-Toc and U0126 blocked AIF release to the cytosolic fraction (*right panel*). *GAPDH*, glyceraldehyde-3-phosphate dehydrogenase.

chondria into the cytosolic fraction of the α-ESA-treated cells, which was in agreement with the findings of microscopic studies (Fig. 4*A*). In addition, manganese superoxide dismutase was detected in the cytosolic fraction 2–7 h after the induction of the cell death (Fig. 4*D*), suggesting that mitochondrial membrane permeabilization occurred in the α-ESA-treated cells. In addition, the increase in the amount of AIF protein in the nucleus is time-dependent. In this fractionation, there was no contamination from the cytosol or heavy membrane fractions. Finally, the inhibitory effect of α-Toc and U0126 on AIF release was investigated. Both α-Toc and U0126 abrogated AIF release.

PARP-1-independent Cell Death—We next found that the α-ESA-mediated cell death was not abrogated by the PARP-1 inhibitor DPQ at concentrations of up to 100 μM. Moreover, no PAR proteins were detected in Western blot analysis (Fig. 5*A*). This suggests that the α-ESA-mediated apoptotic cell death differs not only from caspase-dependent apoptosis but also from caspase-independent and AIF-mediated apoptosis, which always requires PARP-1 activation, as reported elsewhere (29). To our knowledge, no previous report has described AIF-mediated caspase-independent apoptosis without PARP-1 activation.

DNA damage was also evaluated in the α-ESA-treated cells using anti-phosphorylated histone H2AX (γ-H2AX) Ab. Histone H2AX was phosphorylated in response to DNA damages such as double strand breaks by γ-irradiation. The DNA-alkyl-

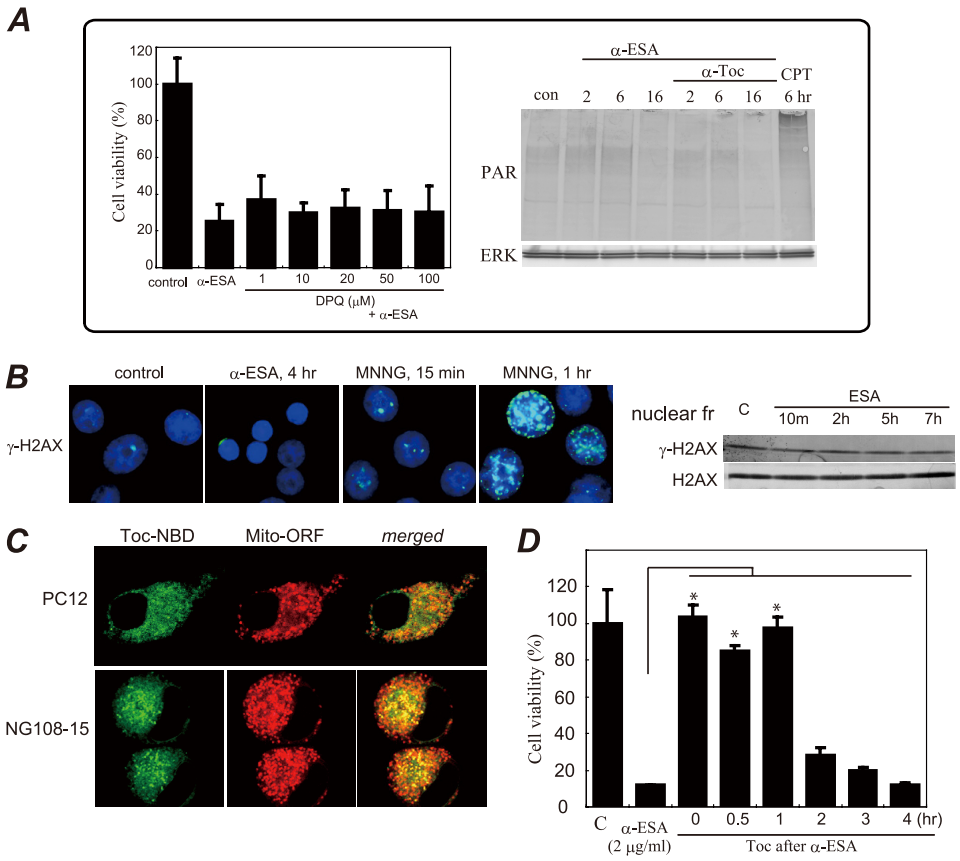

FIGURE 5. *A*, α-ESA-mediated cell death was not inhibited by the established PARP inhibitor DPQ, and PAR proteins were not detected. CPT (40 μM) was used as a positive control for PAR formation. Data were obtained from two independent experiments performed in triplicate (mean ± S.D.). Significance in DPQ-pretreated cells was not observed (*versus* α-ESA alone). *B*, γ-H2AX staining (nuclei in *blue* and γ-H2AX in *green*). Phosphorylation (Ser-139) of histone H2AX (γ-H2AX) was induced by MNNG (500 μM), not by α-ESA (2 μg/ml). γ-H2AX protein levels were not changed in α-ESA-mediated cells. *c*, control. *C*, α-Toc distribution in PC12 and NG108-15 cells was investigated using a confocal microscope. α-Toc is labeled in *green*, and mitochondria are labeled in *red*. The merged images in PC12 and NG108-15 cells show that α-Toc was distributed mostly in the mitochondria. *D*, effect of α-Toc after α-ESA treatment (post-treatment). α-Toc (0.2 μg/ml) was added to the cells at the same time as or after the addition of α-ESA (2 μg/ml). α-Toc blocked cell death 1 h after the addition of α-ESA. Adding α-Toc more than 2 h after α-ESA had no effect. *, $p < 0.05$.

ating agent MNNG induced double strand breaks, whereas α-ESA did not. This indicates that DNA double strand breaks do not arise from the α-ESA-treated cells (Fig. 5*B*).

To clarify the action of α-Toc in these cells, its localization was examined using NBD-labeled α-Toc and orange fluorescent protein-tagged mitochondrial resident protein. In both PC12 and NG108-15 cells, α-Toc mostly migrated to and was localized in the mitochondria (Fig. 5*C*). The localization of α-Toc to the nucleus was not observed in both cell types. The post-treatment with α-Toc 1 h after the addition of α-ESA still blocked the apoptotic cell death (Fig. 5*C*). Recently, ERK1/2 was reported to regulate PARP-1 activation (30, 31). However, PARP-1 itself was not activated in the α-ESA-treated cells.

Microinjection of AIF Antibody—AIF (mouse IgG2b) or MOPC21 (isotype control) antibody was microinjected into the differentiated PC12 cells. The AIF Ab-injected cells blocked the α-ESA-mediated cell death, whereas the MOPC21 Ab-injected cells were killed by α-ESA (Fig. 6*A*). This shows that AIF is a critical factor for the α-ESA-mediated cell death.

Overexpression of Bcl-2—Pro-survival Bcl-2 widely protects apoptosis induced by various stimuli such as camptothecin, etoposide, and staurosporine because Bax/Bak-mediated release of Cyt-c, Smac/Diablo, AIF from mitochondria is blocked by pro-apoptotic Bcl-2 and Bcl-X_L (9, 32, 33). Thus, PC12 cells were transfected with *bcl-2* by the electroporation method (Amaxa Nucleofector II). The amount of Bcl-2 protein in the transfected cells was approximately nine times greater than that in mock-transfected cells according to Western blot analysis. The cell viability was measured using the WST-8 assay reagent for the whole cells. The release of AIF from the mitochondria to the nucleus was suggested to be regulated by Bcl-2 (34). However, the α-ESA-mediated apoptotic cell death was not blocked by Bcl-2 overexpression (Fig. 6*B*). Yu *et al.* (20) reported that Bcl-2 alone was not sufficient to prevent MNNG-treated AIF release and caspase-independent cell death.

RNA Interference of PARP-1 or MEK1/2—α-ESA induced AIF release, resulting in the cell death without PARP-1 activation. The well established PARP-1 inhibitor DPQ did not block the apoptotic cell death. To clarify the involvement of PARP-1 in the α-ESA-mediated cell death, the knockdown experiments for PARP-1 were carried out using siRNA targeted for rat PARP-1. The siRNA-transfected PC12 cells were exposed to α-ESA (2 μg/ml) or MNNG (500 μM) as a positive control in the differentiated condition. The PARP-1 knockdown inhibited the MNNG-treated cell death, whereas the knockdown did not abrogate the α-ESA-mediated cell death (Fig. 6*C*). DPQ treatment of PARP-1 knockdown cells also did not block the cell death (Fig. 6*D*). These results suggest that PARP-1, which is considered to be required for AIF-initiated caspase-independent apoptosis, is not involved in the α-ESA-mediated cell death.

We next investigated whether or not ERK1/2 phosphorylation was critical for the α-ESA-mediated cell death using siRNA targeted for rat MEK1/2. The siRNAs for MEK1 or MEK2 were transfected into PC12 cells, and the cells were exposed to α-ESA (5 μg/ml) in the proliferation condition. The knockdown of either MEK1 or MEK2 effectively blocked the α-ESA-mediated cell death (Fig. 6*E*). Together with the inhibitor (U0126) experiments, these results indicate that ERK1/2 phosphorylation plays an important role in the α-ESA-mediated apoptotic cell death.

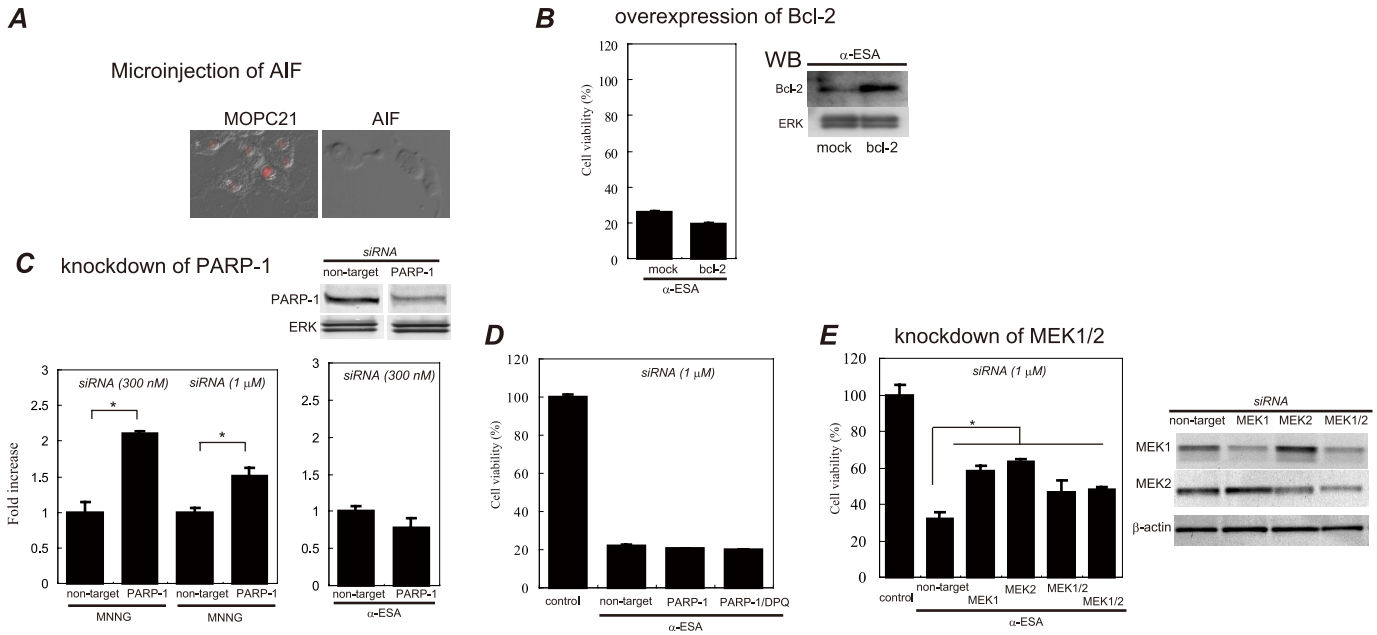

FIGURE 6. **Effect of AIF microinjection, Bcl-2 overexpression, and knockdown of PARP-1 and MEK1/2 on α-ESA-mediated apoptosis.** *A,* microinjection of AIF antibody blocks α-ESA-mediated apoptosis. AIF or MOPC21 (isotype control) antibody (*Ab*) was microinjected into the differentiated PC12 cells using Stamporation apparatus and incubated for 6 h. The cells were exposed to α-ESA (2 μg/ml) for 16 h and stained with propidium iodide. The AIF Ab-microinjected cells blocked α-ESA-mediated cell death, whereas the MOPC21 Ab-microinjected cells did not, stained in *red*, which means the cells were dead. Images were obtained from three independent experiments. All cells in these images were microinjected. *B, bcl-2* was transiently transfected into PC12 cells. After 24 h of incubation, the cells were exposed to α-ESA (2 μg/ml) and incubated for another 16 h. The cell viability was measured for the whole cells. The overexpression of Bcl-2 did not protect PC12 cells from α-ESA-mediated apoptosis ($n = 3$). *WB*, Western blot. *C,* siRNA targeted for rat PARP-1 was transfected into PC12 cells. After 24 h of incubation, the cells were exposed to α-ESA (2 μg/ml) or MNNG (500 μM) and incubated for another 16 h. The cell viability was measured for the whole cells. The knockdown of PARP-1 did not block α-ESA-mediated apoptosis, whereas it prevented MNNG-treated (500 μM, 15 min) cells from the apoptosis. ($n = 3$; *, $p < 0.001$). *D,* combination of PARP-1 knockdown and DPQ treatment (50 μM) had no effect on the block of the apoptosis. *E,* siRNA experiments for rat MEK1 and MEK2 were performed in the proliferation condition. The knockdown of either MEK1 or MEK2 significantly blocked α-ESA-mediated cell death ($n = 6$; *, $p < 0.05$). The knockdown of both MEK1 and MEK2 also inhibited the cell death. The transfection efficiency was ~80% judging from the cells transfected with cDNA encoding green fluorescent protein. The blots for the knockdown samples are shown in the *right panel*. The cell viabilities were measured for the whole cells in overexpression and knockdown experiments.

Involvement of Superoxide Anion Radicals and Mitochondrial Membrane Potential in α-ESA-mediated Cell Death—Involvement of ROS in the α-ESA-mediated apoptotic cell death was next investigated using fluorescent probes, CM-5-(and-6)-chloromethyl-2′,7′-dichlorodihydrofluorescein diacetate for total ROS and BESSo-AM (35, 36) and MitoSOX Red for superoxide anion radicals. Intracellular ROS was observed in the α-ESA-treated cells. The ROS production was blocked by α-Toc pretreatment, whereas epicatechin was not able to inhibit ROS production and the apoptotic cell death (Fig. 7*A*). Superoxide anion radicals were produced shortly before the α-ESA-mediated plasma membrane blebbing started (Fig. 7*B*). Some BESSo-positive cells showed normal morphology, and some of the cells started plasma membrane blebbing. The production of superoxide anion radicals was time-dependent. The strongest intensity was observed 5 h after α-ESA treatment. Superoxide anion radicals produced by α-ESA are probably a small quantity because a trace amount of α-Toc (0.01 μg/ml) localized mostly in the mitochondria abrogated the apoptotic cell death. It appears that the α-ESA-mediated cell death is different from that induced by a high concentration of 1-methyl-4-phenylpyridine or 3-nitropropionic acid (>1 mM), which can produce a large amount of ROS and activate caspase. Superoxide production was also measured using MitoSOX Red to detect superoxides in the mitochondria. Superoxide was produced in the α-ESA-treated cells, whereas the cells pretreated with α-Toc scavenged superoxides (Fig. 7*C*). U0126 almost blocked superoxides.

Mitochondrial membrane potential ($\Delta\Phi_m$) was next examined using JC-1 staining. An uncoupler, carbonyl cyanide *p*-chlorophenylhydrazone, in the mitochondria-electron transport chain immediately abrogated the potential. In contrast, the mitochondrial membrane potential gradually decreased over 5 h in the α-ESA-treated cells (Fig. 7*D*). These results suggest that α-ESA initiates a small amount of superoxide anion radicals, thereby inducing the reduction in the mitochondrial membrane potential, which results in the cell death associated with the plasma membrane blebbing.

Bax Localization of α-ESA-mediated Cells—In the STS-treated cells, Bax started to translocate into the mitochondria at 4 h. However, Bax migration to the mitochondria was not observed in the α-ESA-mediated cells (Fig. 8). These results suggest that Bax-induced channel formation in the mitochondrial outer membrane is not involved in the α-ESA-mediated cell death. The data that Cyt-c was not released from the mitochondria into the cytosol before AIF (Fig. 4*D*) support this result.

Putative Cell Death Mechanism Induced by α-ESA—When cells were treated with STS or actinomycin D in the presence of Z-VAD-fmk, caspase activation was blocked. However, Bax and Bak are localized in the mitochondria, resulting in the release of Cyt-c, AIF, and other mitochondrial proteins such as Smac/

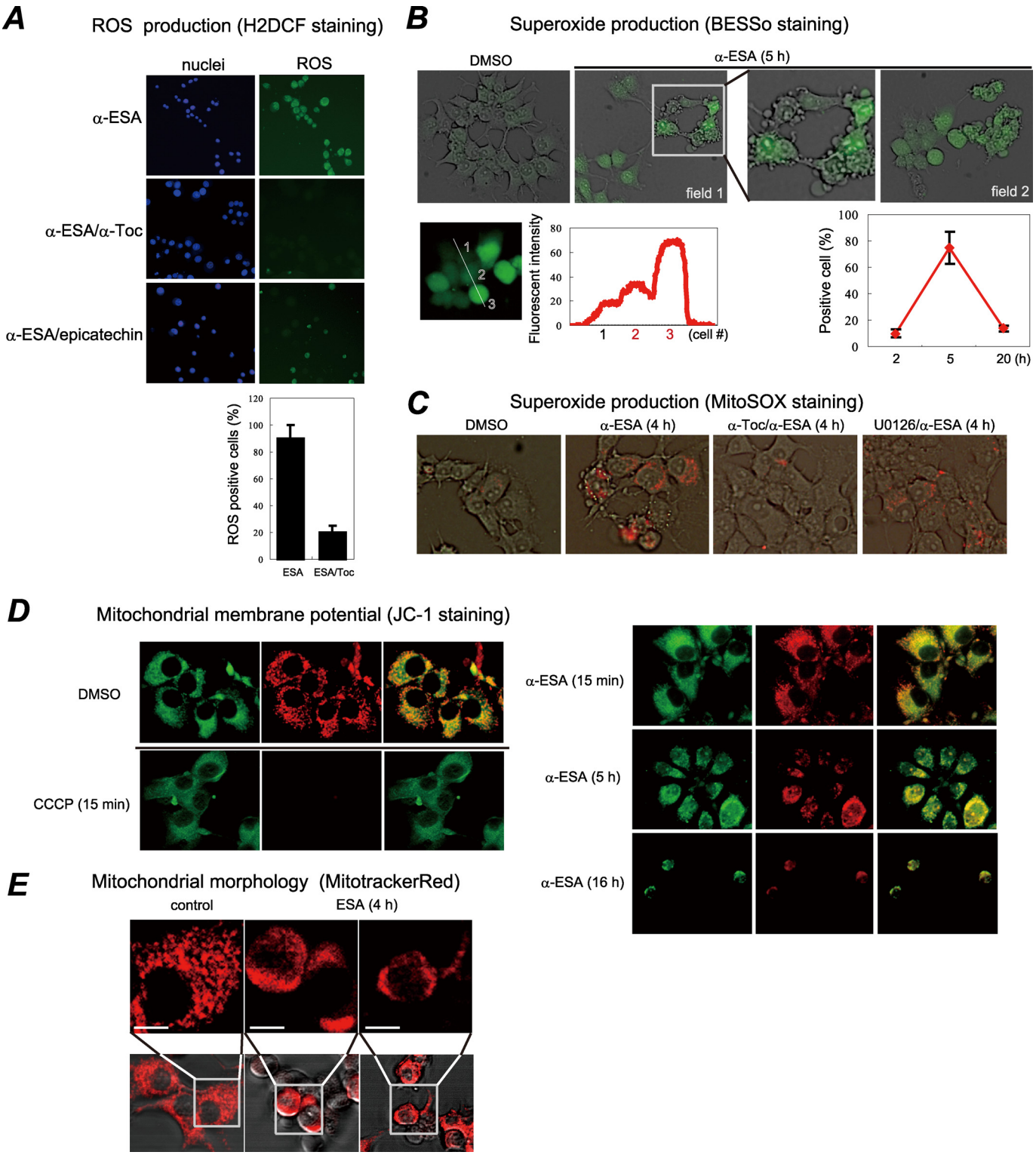

FIGURE 7. **Production of ROS and mitochondrial membrane potential in α-ESA-treated cells.** *A*, intracellular total ROS was measured using H2DCF fluorescent probe. α-ESA initiated ROS, which was blocked by α-Toc (2 μg/ml) but not epicatechin (20 μM). The numbers of ROS-positive cells were counted in the α-ESA-treated cells (12 h) with or without α-Toc. *B*, production of superoxide anion radicals (O_2^-) was measured using BESSo fluorescent probe, specific for O_2^-. Fluorescent intensities were analyzed by ImageJ software. The cell numbers 2 and 3 that have fluorescent intensities more than the signal to noise ratio of >5 were positive. O_2^- production was observed 5 h after the addition of α-ESA (*bottom right*). Membrane blebbing was observed immediately after superoxide production. *C*, O_2^- was measure by MitoSOX Red indicator. O_2^- was produced in α-ESA-treated cells. α-Toc (2 μg/ml) inhibited the O_2^- production. U0126 (5 μM) almost blocked the O_2^- production. *D*, mitochondrial membrane potential was measured using JC-1. Carbonyl cyanide *p*-chlorophenylhydrazone (*CCCP*) (50 μM) immediately shut down the potential. α-ESA gradually reduced the potential. *E*, mitochondrial morphology during α-ESA-mediated cell death process. Fragmented and condensed mitochondria were observed in the α-ESA-treated cells. *Scale bars* show 8 μm.

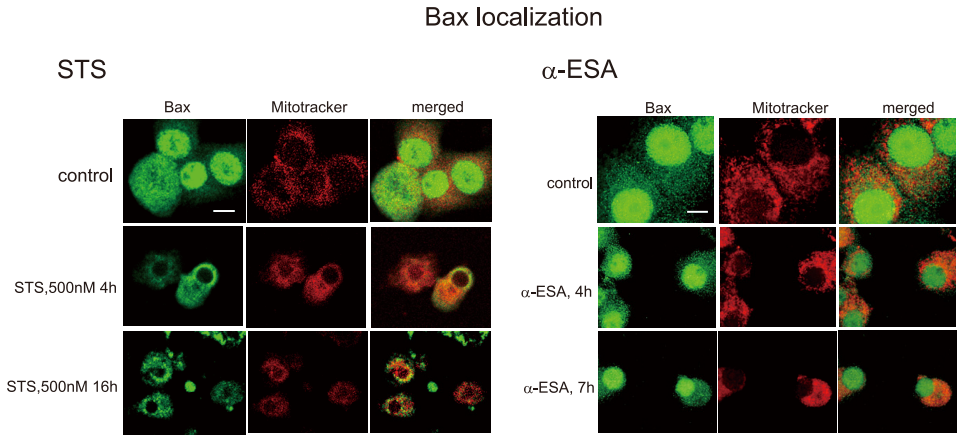

FIGURE 8. **Bax localization of α-ESA-treated cells.** The differentiated PC12 cells were treated with staurosporine (1 μM) or α-ESA (2 μg/ml), and stained with anti-Bax and MitoTracker Red CM-H2Ros. Bax migrated into the mitochondria in the STS-treated cells, whereas Bax did not in the α-ESA-treated cells.

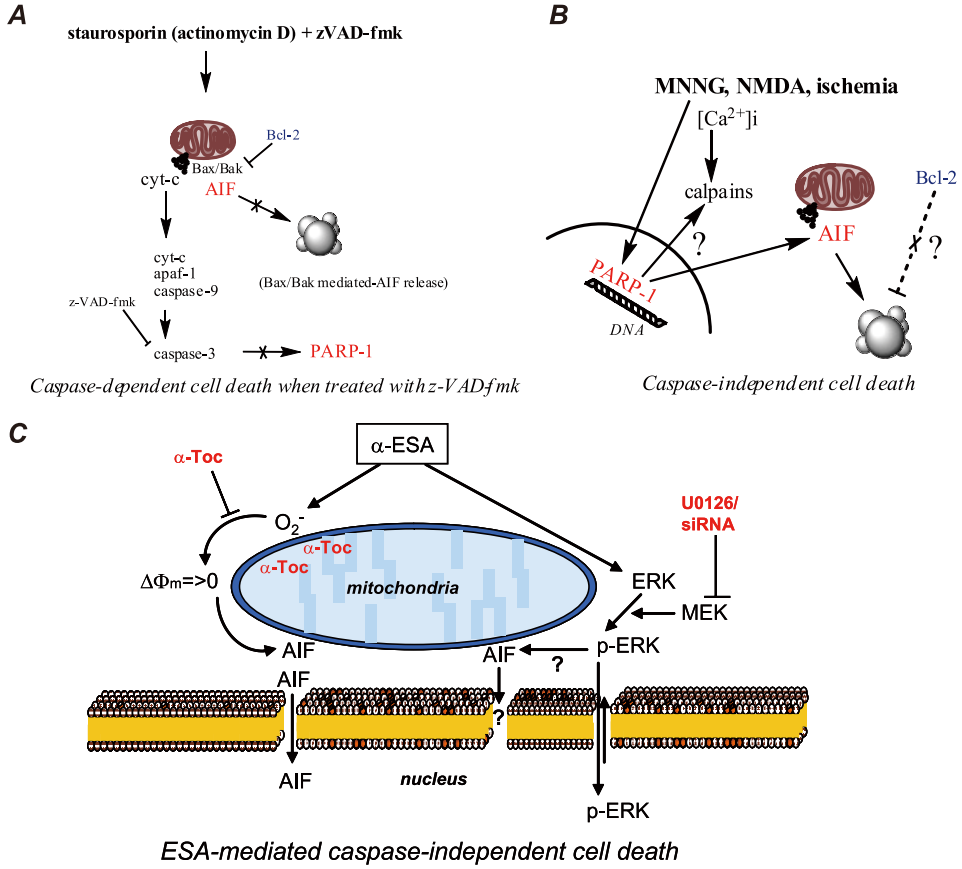

FIGURE 9. **A speculative mechanism of α-ESA-mediated cell death.** *A,* staurosporine + Z-VAD-fmk treatment induces Bax/Bak-mediated Cyt-c, AIF, and other apoptotic mitochondrial proteins such Smac/Diablo, although caspase is blocked by Z-VAD-fmk. This type of apoptosis is blocked by pro-survival Bcl-2 protein. *B,* MNNG, NMDA, or hypoxia ischemia induces the increase in an intracellular Ca^{2+} concentration ($[Ca^{2+}]_i$), intracellular ROS production, and DNA alkylation followed by PARP-1 activation, which results in PARP-1-mediated AIF release, leading to the caspase-independent cell death. *C,* α-ESA induces PARP-1-independent AIF-release, resulting in a novel caspase-independent apoptosis. U0126 and MEK1/2 knockdown block the cell death by unknown mechanisms. ERK1/2 is certainly involved in the cell death. α-Toc blocks ROS production in the mitochondria and cell death without the influence on ERK1/2. PARP-1 is not involved in α-ESA-mediated cell death. α-ESA appears to act separately on MEK1/2-ERK1/2 and superoxide production leading to the reduction of the membrane potential.

Diablo, Omi/HtrA2 (Fig. 9*A*). The excitotoxic NMDA or DNA-alkylating agent MNNG induces DNA damage leading to PARP-1 activation, which results in PARP-1-dependent AIF release and cell death (Fig. 9*B*). In caspase-independent apoptosis, PARP-1 is believed to be a death signal. On the other hand, α-ESA induces PARP-1-independent AIF release through the production of superoxide and ERK1/2 phosphorylation, resulting in caspase-independent and PARP-1-independent cell death (Fig. 9*C*). α-Toc protects the α-ESA-mediated cell death because mitochondrially localized α-Toc can scavenge superoxides. This is a novel and alternative pathway for caspase-independent apoptosis without the involvement of other apoptotic proteins.

DISCUSSION

α-ESA is a conjugated trienoic fatty acid and an isomer of nonconjugated linolenic acid. It has been reported to suppress both tumor growth *in vivo* and angiogenesis *in vitro* by inducing caspase-3 via lipid peroxidation at a concentration of 20 μM (23, 24). α-ESA has been shown to be cytotoxic in human tumor cell lines such as DLD-1, HepG2, and A549, although MCF-7 cells lacking caspase-3 were relatively resistant to the α-ESA-mediated apoptosis (22). These reports suggest that a higher concentration of α-ESA can activate caspase-dependent pathways in non-neuronal cells.

First of all, in this study apoptosis induced by α-ESA was not blocked by both the broad spectrum caspase inhibitor Z-VAD-fmk and caspase-3 inhibitor, but it was inhibited by the MEK inhibitor U0126 and the lipophilic antioxidant α-Toc. The α-ESA-mediated apoptosis was abrogated by as little as 23 nM (0.01 μg/ml) of α-Toc. If the peroxidation of α-ESA is involved in the α-ESA-mediated neuronal death, a similar molar concentration of antioxidants should be needed to protect the cells. In addition, intracellular ROS production caused by the peroxidation of α-ESA can deactivate phosphatases by the oxidation in the active center, leading to the increase in ERK1/2 phosphorylation. This phosphorylation can be inhibited by antioxidants. However, α-Toc did not block the increase in ERK1/2 phosphorylation. Even when α-Toc was

added to the cells 1 h after treatment with α-ESA, it blocked the α-ESA-mediated cell death. Moreover, the cell death was not mediated by α-ESA-Me (methyl ester of α-ESA). Together with MitoSOX Red analysis, these results suggest that α-Toc blocks the α-ESA-mediated superoxide production in a small quantity at least in the mitochondria and the resulting cell death.

α-Toc reportedly up-regulated pro-survival Bcl-2 and protected against hydrogen peroxide (H_2O_2)-induced cell death in cortical neurons 24 h after pretreatment with 10 nM α-Toc through ERK1/2 activation (37). The amount of Bcl-2 protein was not changed in this study.[3] Thus, the effect of α-Toc on the up-regulation of Bcl-2 is not important in this apoptotic cell death. This is supported by Bcl-2 overexpression study.

Second, U0126 completely prevented the α-ESA-mediated cell death. U0126 blocked the migration of AIF. The knockdown experiments of MEK1 and MEK2 revealed that MEK1/2 is an important pathway in the α-ESA-mediated cell death.

Caspase-3 and PARP-1 were not activated by α-ESA during the apoptotic cell death process. PARP-1 activation followed by AIF migration is considered to be important for caspase-independent apoptotic cell death. In this study, AIF was released from the mitochondria and migrated to the nucleus by α-ESA. By 7 h, the nucleus was condensed, and AIF was localized throughout the nucleus. However, the cell death was not inhibited by the PARP-1 inhibitor DPQ. PAR proteins were not observed in α-ESA-treated cells at various time points. In addition, PARP-1 knockdown had no protective effect on the α-ESA-mediated cell death. The combination of PARP-1 knockdown and DPQ pretreatment showed no effect. The PAR polymer is considered to be a death signal. AIF is thought to be mediated by PARP-1 activation in caspase-independent apoptotic cells (21, 29, 38, 39). To our knowledge, these are the novel findings of AIF-mediated and caspase-independent apoptosis without PARP-1 activation.

Third, STS or actinomycin D in the presence of Z-VAD-fmk may induce apoptosis without activation of caspase and PARP-1. However, Bax already migrated to the mitochondria to form Bax/Bak channels to release apoptotic proteins such as Cyt-c, AIF, and Smac/Diablo. Bax was not translocated to the mitochondria in the α-ESA-treated cells, whereas Bax did migrate to the mitochondria in the STS-treated cells. Moreover, Cyt-c was not released into the cytosol before AIF. These results suggest that Bax-mediated apoptosis is not involved in the α-ESA-mediated apoptosis. Thus, this type of pathway is excluded. In addition, manganese superoxide dismutase was released into the cytosol, suggesting mitochondrial remodeling or membrane permeabilization associated with the reduction of mitochondrial membrane potential during the apoptotic process, independently of PARP-1 and other signaling molecules. Scattered and condensed mitochondria were observed (Fig. 7*E*).

Fourth, ERK1/2 is reportedly activated by CPT, etoposide (40), and MNNG (31). The apoptotic cell death induced by etoposide and MNNG can be blocked by MEK1/2 inhibitors PD98059 and U0126, the latter of which protects against brain ischemia (41). These reports suggest that ERK1/2 is a key regulator of apoptosis (42). Kauppinen *et al.* (31) reported on the regulation of PARP-1 by ERK1/2 and the inhibition of neuronal cell death by DPQ. However, DPQ at concentrations of up to 100 μM was unable to prevent the cells from the α-ESA-mediated apoptosis. MNNG or NMDA induces PARP-1-dependent AIF translocation to the nucleus. Thus, MNNG or NMDA-treated and the α-ESA-treated cells appear to exert different signaling pathways. Calpain I can mediate AIF release from the mitochondria in ischemia neuronal injury (43). Moubarak *et al.* (21) reported that PARP-1 was activated upstream of calpains in MNNG-induced murine embryo fibroblasts. Recently, however, calpain was reported to be unnecessary for AIF translocation in PARP-1-dependent cell death (44). In this study, the α-ESA-mediated cell death was not abrogated by the calpain inhibitors *N*-Acetyl-Leu-Leu-Nle-CHO ALLN and calpeptin and by the Ca^{2+}-dependent- and independent phospholipase A_2 inhibitors, bromoenol lactone, methylarachidonyl fluorophosphonate (MAFP), and palmitoyl trifluoromethyl ketone.

MNNG, NMDA, or hypoxia ischemia can all induce oxidative stress, thereby leading to DNA damage. These stimuli can initiate caspase-independent and PARP-1-dependent signaling cascades. In contrast, α-ESA did not activate PARP-1, although the α-ESA-treated cells became TUNEL-positive. H2AX was not phosphorylated by α-ESA, indicating that DNA strand breaks did not occur. The overexpression of Bcl-2 did not block the α-ESA-mediated apoptotic cell death. Bcl-2 appears not to be enough to protect against α-ESA-mediated apoptosis.

In conclusion, our results show that α-ESA causes a novel PARP-1-independent AIF release and the cell death through the superoxide production and the prolonged ERK1/2 phosphorylation. The cell death was not associated with Bax, Cyt-c, caspase-3, and PARP-1.

Acknowledgments—We thank S. Tanaka for performing the confocal microscopic studies and M. Soga for performing the deconvolution microscopic studies.

REFERENCES

1. Kerr, J. F., Wyllie, A. H., and Currie, A. R. (1972) *Br. J. Cancer* **26,** 239–257
2. Nagata, S. (1997) *Cell* **88,** 355–365
3. Ashkenazi, A., and Dixit, V. M. (1998) *Science* **281,** 1305–1308
4. Evan, G., and Littlewood, T. (1998) *Science* **281,** 1317–1322
5. Taylor, R. C., Cullen, S. P., and Martin, S. J. (2008) *Nat. Rev. Mol. Cell Biol.* **9,** 231–241
6. Eguchi, Y., Ewert, D. L., and Tsujimoto, Y. (1992) *Nucleic Acids Res.* **20,** 4187–4192
7. Okuno, S., Shimizu, S., Ito, T., Nomura, M., Hamada, E., Tsujimoto, Y., and Matsuda, H. (1998) *J. Biol. Chem.* **273,** 34272–34277
8. Tsujimoto, Y. (2003) *J. Cell. Physiol.* **195,** 158–167
9. Youle, R. J., and Strasser, A. (2008) *Nat. Rev. Mol. Cell Biol.* **9,** 47–59
10. Pettmann, B., and Henderson, C. E. (1998) *Neuron* **20,** 633–647
11. Chen, J., Nagayama, T., Jin, K., Stetler, R. A., Zhu, R. L., Graham, S. H., and Simon, R. P. (1998) *J. Neurosci.* **18,** 4914–4928
12. Graham, S. H., and Chen, J. (2001) *J. Cereb. Blood Flow Metab.* **21,** 99–109
13. Lorenzo, H. K., Susin, S. A., Penninger, J., and Kroemer, G. (1999) *Cell Death Differ.* **6,** 516–524
14. Susin, S. A., Lorenzo, H. K., Zamzami, N., Marzo, I., Snow, B. E., Brothers, G. M., Mangion, J., Jacotot, E., Costantini, P., Loeffler, M., Larochette, N., Goodlett, D. R., Aebersold, R., Siderovski, D. P., Penninger, J. M., and Kroemer, G. (1999) *Nature* **397,** 441–446
15. Cregan, S. P., Fortin, A., MacLaurin, J. G., Callaghan, S. M., Cecconi, F., Yu, S. W., Dawson, T. M., Dawson, V. L., Park, D. S., Kroemer, G., and Slack, R. S. (2002) *J. Cell Biol.* **158,** 507–517

16. Wang, H., Yu, S. W., Koh, D. W., Lew, J., Coombs, C., Bowers, W., Federoff, H. J., Poirier, G. G., Dawson, T. M., and Dawson, V. L. (2004) *J. Neurosci.* **24,** 10963–10973
17. Zhu, C., Wang, X., Huang, Z., Qiu, L., Xu, F., Vahsen, N., Nilsson, M., Eriksson, P. S., Hagberg, H., Culmsee, C., Plesnila, N., Kroemer, G., and Blomgren, K. (2007) *Cell Death Differ.* **14,** 775–784
18. Zhu, C., Qiu, L., Wang, X., Hallin, U., Candé, C., Kroemer, G., Hagberg, H., and Blomgren, K. (2003) *J. Neurochem.* **86,** 306–317
19. Zhang, X., Chen, J., Graham, S. H., Du, L., Kochanek, P. M., Draviam, R., Guo, F., Nathaniel, P. D., Szabó, C., Watkins, S. C., and Clark, R. S. (2002) *J. Neurochem.* **82,** 181–191
20. Yu, S. W., Wang, H., Poitras, M. F., Coombs, C., Bowers, W. J., Federoff, H. J., Poirier, G. G., Dawson, T. M., and Dawson, V. L. (2002) *Science* **297,** 259–263
21. Moubarak, R. S., Yuste, V. J., Artus, C., Bouharrour, A., Greer, P. A., Menissier-de Murcia, J., and Susin, S. A. (2007) *Mol. Cell. Biol.* **27,** 4844–4862
22. Igarashi, M., and Miyazawa, T. (2000) *Cancer Lett.* **148,** 173–179
23. Tsuzuki, T., Tokuyama, Y., Igarashi, M., and Miyazawa, T. (2004) *Carcinogenesis* **25,** 1417–1425
24. Tsuzuki, T., and Kawakami, Y. (2008) *Carcinogenesis* **29,** 797–806
25. Hara, C., Tateyama, K., Akamatsu, N., Imabayashi, H., Karaki, K., Nomura, N., Okano, H., and Miyawaki, A. (2006) *Brain Cell Biol.* **35,** 229–237
26. Sasagawa, S., Ozaki, Y., Fujita, K., and Kuroda, S. (2005) *Nat. Cell Biol.* **7,** 365–373
27. Santos, S. D., Verveer, P. J., and Bastiaens, P. I. (2007) *Nat. Cell Biol.* **9,** 324–330
28. Susin, S. A., Daugas, E., Ravagnan, L., Samejima, K., Zamzami, N., Loeffler, M., Costantini, P., Ferri, K. F., Irinopoulou, T., Prévost, M. C., Brothers, G., Mak, T. W., Penninger, J., Earnshaw, W. C., and Kroemer, G. (2000) *J. Exp. Med.* **192,** 571–580
29. Andrabi, S. A., Kim, N. S., Yu, S. W., Wang, H., Koh, D. W., Sasaki, M., Klaus, J. A., Otsuka, T., Zhang, Z., Koehler, R. C., Hurn, P. D., Poirier, G. G., Dawson, V. L., and Dawson, T. M. (2006) *Proc. Natl. Acad. Sci. U.S.A.* **103,** 18308–18313
30. Cohen-Armon, M., Visochek, L., Rozensal, D., Kalal, A., Geistrikh, I., Klein, R., Bendetz-Nezer, S., Yao, Z., and Seger, R. (2007) *Mol. Cell* **25,** 297–308
31. Kauppinen, T. M., Chan, W. Y., Suh, S. W., Wiggins, A. K., Huang, E. J., and Swanson, R. A. (2006) *Proc. Natl. Acad. Sci. U.S.A.* **103,** 7136–7141
32. Shimizu, S., Eguchi, Y., Kosaka, H., Kamiike, W., Matsuda, H., and Tsujimoto, Y. (1995) *Nature* **374,** 811–813
33. Yang, J., Liu, X., Bhalla, K., Kim, C. N., Ibrado, A. M., Cai, J., Peng, T. I., Jones, D. P., and Wang, X. (1997) *Science* **275,** 1129–1132
34. Otera, H., Ohsakaya, S., Nagaura, Z., Ishihara, N., and Mihara, K. (2005) *EMBO J.* **24,** 1375–1386
35. Maeda, H., Yamamoto, K., Kohno, I., Hafsi, L., Itoh, N., Nakagawa, S., Kanagawa, N., Suzuki, K., and Uno, T. (2007) *Chemistry* **13,** 1946–1954
36. Maeda, H., Yamamoto, K., Nomura, Y., Kohno, I., Hafsi, L., Ueda, N., Yoshida, S., Fukuda, M., Fukuyasu, Y., Yamauchi, Y., and Itoh, N. (2005) *J. Am. Chem. Soc.* **127,** 68–69
37. Numakawa, Y., Numakawa, T., Matsumoto, T., Yagasaki, Y., Kumamaru, E., Kunugi, H., Taguchi, T., and Niki, E. (2006) *J. Neurochem.* **97,** 1191–1202
38. Culmsee, C., Zhu, C., Landshamer, S., Becattini, B., Wagner, E., Pellecchia, M., Pellechia, M., Blomgren, K., and Plesnila, N. (2005) *J. Neurosci.* **25,** 10262–10272
39. Yu, S. W., Andrabi, S. A., Wang, H., Kim, N. S., Poirier, G. G., Dawson, T. M., and Dawson, V. L. (2006) *Proc. Natl. Acad. Sci. U.S.A.* **103,** 18314–18319
40. Tang, D., Wu, D., Hirao, A., Lahti, J. M., Liu, L., Mazza, B., Kidd, V. J., Mak, T. W., and Ingram, A. J. (2002) *J. Biol. Chem.* **277,** 12710–12717
41. Namura, S., Iihara, K., Takami, S., Nagata, I., Kikuchi, H., Matsushita, K., Moskowitz, M. A., Bonventre, J. V., and Alessandrini, A. (2001) *Proc. Natl. Acad. Sci. U.S.A.* **98,** 11569–11574
42. Subramaniam, S., Zirrgiebel, U., von Bohlen Und Halbach, O., Strelau, J., Laliberté, C., Kaplan, D. R., and Unsicker, K. (2004) *J. Cell Biol.* **165,** 357–369
43. Cao, G., Xing, J., Xiao, X., Liou, A. K., Gao, Y., Yin, X. M., Clark, R. S., Graham, S. H., and Chen, J. (2007) *J. Neurosci.* **27,** 9278–9293
44. Wang, Y., Kim, N. S., Li, X., Greer, P. A., Koehler, R. C., Dawson, V. L., and Dawson, T. M. (2009) *J. Neurochem.* **110,** 687–696